



# Development of nanoparticle sizing system using fluorescence polarization

Terutake Hayashi, Masaki Michihata, Yasuhiro Takaya, Kok Foong Lee

Osaka University, 2-1 Yamadaoka, Suita, Osaka 565-0871, Japan

## ABSTRACT

To measure the sizes of nanoparticles with a wide size distribution in a solvent, we developed an optical microscopy system that enables fluorescence polarization (FP) measurement and optical observation. This system allows the evaluation of nanoparticle sizes over a wide range because the fluorescence signal intensity is independent of changes in the nanoparticle sizes. In this paper, we describe a fundamental experiment to verify the feasibility of using this system for different sizes of nanoparticles.

**Section:** RESEARCH PAPER

**Keywords:** nanoparticle; fluorescence polarization; Brownian motion; rotational diffusion coefficient; particle sizing

**Citation:** Terutake Hayashi, Masaki Michihata, Yasuhiro Takaya, Kok Foong Lee, Development of nanoparticle sizing system using fluorescence polarization, Acta IMEKO, vol. 2, no. 2, article 12, December 2013, identifier: IMEKO-ACTA-02 (2013)-02-12

**Editor:** Paolo Carbone, University of Perugia

**Received** April 15<sup>th</sup>, 2013; **In final form** November 17<sup>th</sup>, 2013; **Published** December 2013

**Copyright:** © 2013 IMEKO. This is an open-access article distributed under the terms of the Creative Commons Attribution 3.0 License, which permits unrestricted use, distribution, and reproduction in any medium, provided the original author and source are credited

**Funding:** This work was supported in part by a Grant-in-Aid for Scientific Research from the Ministry of Education, Culture, Sports, Science and Technology of Japan (Grant-in-Aid for Exploratory Research 21686015).

**Corresponding author:** Terutake Hayashi, e-mail: hayashi@mech.eng.osaka-u.ac.jp

## 1. INTRODUCTION

The integration of nanoparticles into devices produces unique electronic, photonic, and catalytic properties. It offers the prospect of both new fundamental scientific advances and useful technological applications. Many of the fundamental properties of materials (e.g., optical, electrical, and mechanical) can be expressed as functions of the size, shape, composition, and structural order [1, 2]. It is important to evaluate nanoparticle sizes and maintain a constant state (size distribution, average size, shape uniformity).

The size distribution of monodispersed nanoparticles in a solvent can be measured using dynamic light scattering [3, 4]. However, the scattering method is inappropriate for detecting the sizes of particles in a mixture, which include both small monodispersed particles and large particles such as agglomerates. The signal intensity depends on the sixth power of the particle diameter. Therefore, the scattering signal from monodispersed particles, compared to the signal from their agglomerates, is too small to detect.

The size distribution of nanoparticles with a wide size distribution can be measured using transmission electron microscopy [5]. This requires a dried sample. However, it is difficult to evaluate both the average diameter and size

distribution of nanoparticles because of the instability of their diameters in a solvent.

To measure the sizes of nanoparticles with a wide size distribution in a solvent, we developed an optical microscopy system that enables fluorescence polarization (FP) measurement and optical observation. The FP method can trace the rotational diffusion constant of Brownian motion in a fluorescent molecule. When a fluorophore is used to label nanoparticles, the rotational diffusion coefficient corresponds to the size of the nanoparticles. The system makes it possible to evaluate nanoparticle sizes over a wide range because the fluorescence signal intensity is independent of changes in the nanoparticle sizes. In this paper, we describe a fundamental experiment to verify the feasibility of using this method for different sizes of nanoparticles.

## 2. MEASUREMENT OF ROTATIONAL DIFFUSION COEFFICIENT AND PARTICLE SIZING

### 2.1. Measurement of rotational diffusion coefficient

We have developed an FP method [6, 7, 8] to measure nanoparticle sizes by measuring the rotational diffusion coefficient. When linearly polarized light is irradiated on a nanoparticle labeled with a fluorophore, a fluorescence signal

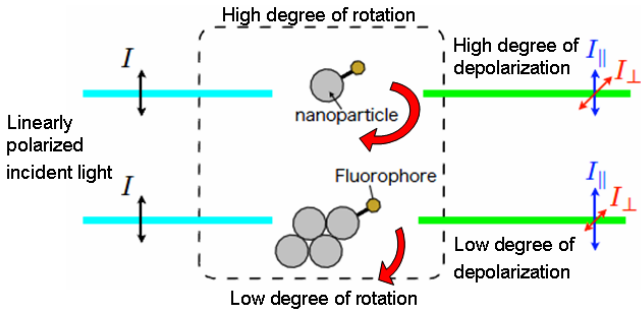


Figure 1. Concept of fluorescence polarization method.

initially maintains the polarization state of the irradiation light. As shown in Figure 1, small particles will have a high degree of rotation due to Brownian motion, and the polarization plane of the light emitted will vary greatly from that of the excitation light. In contrast, larger particles will have a low degree of rotation, so light is emitted in the polarized plane, similar to the excitation light. The fluorescence signal then depolarizes as time passes. The fluorescence anisotropy depends on the angle of the particle rotation. In addition, depolarization is rapid for particles with small volumes, whereas the polarization state is maintained longer in particles with large volumes.

The fluorescence anisotropy  $r(t)$  is related to the rotational diffusion coefficient  $D_r$  of a nanoparticle. The particle size can be calculated from  $D_r$  on the basis of an analysis using the Debye–Stokes–Einstein (DSE) relationship [8, 9] when the particle shape is approximated to that of a sphere. Here  $r(t)$  is defined by

$$r(t) = \frac{I_{\parallel} - I_{\perp}}{I_{\parallel} + 2I_{\perp}} \quad (1)$$

where the first and second subscripts refer to the orientation of the excitation and that of the emission, respectively.  $I_{\parallel}$  and  $I_{\perp}$  are the horizontally polarized (p-polarized) and vertically polarized (s-polarized) components of the fluorescence, respectively, when horizontally polarized light is irradiated.

We can also express  $r(t)$  as a function of time  $t$  as

$$r(t) = (r_0 - r_{\infty})e^{-t/\theta} + r_{\infty} \quad i(t) = \frac{e^{-t/\tau}}{\tau} \quad (2)$$

where  $i(t)$  is the instantaneous emission intensity normalized to a unit-integrated value. The parameter  $r_{\infty}$  reflects the extent of the rotational reorientation of the fluorophore. In this case,  $\bar{r}$  is obtained by integrating the intensity-weighted  $r(t)$ , as shown in Eq. (3).

The steady-state anisotropy  $\bar{r}$  of a fluorophore undergoing isotropic rotational diffusion is related to the fluorescence lifetime,  $\tau$  and rotational correlation time  $\theta$  [4]:

$$\bar{r} = \int_0^{\infty} r(t) \cdot i(t) dt \Leftrightarrow \frac{r_0 - r_{\infty}}{\bar{r} - r_{\infty}} = 1 + \sigma \quad (3)$$

where  $r_0$  is a limiting value in the absence of rotation given by the relative orientation of the absorption and emission transition moments, and  $\sigma$  is the ratio  $\theta/\tau$ .

Measurements of the anisotropy decay can reveal a multiplicity of rotational correlation times reflecting heterogeneity in the size, shape, and internal motions of the fluorophore–nanoparticle conjugate. The rotational correlation

times are determined in either the time domain or the frequency domain. The rotational diffusion coefficient can be precisely calculated from the fluorescence anisotropy in the frequency domain. When an excitation pulse is used as a forcing function, Eq. (3) is transformed into a decay process in which the fluorescence lifetime  $\tau$  is no longer linked to the correlation time.

The rotational correlation times are determined by measuring three parameters:  $\Phi$ ,  $Y_{AC}$ , and  $Y_{DC}$ . To define them, we measure the sinusoidal waveforms of both  $I_{\parallel}$  and  $I_{\perp}$  in the frequency domain. A series of  $I_{\parallel}$  and  $I_{\perp}$  are measured while the relative phase between the excitation light and the detector gain is adjusted as the excitation light and detector gain are modulated using the same radial frequency.

After the sinusoidal signals of  $I_{\parallel}$  and  $I_{\perp}$  are acquired, each data set is processed to yield the frequency-dependent amplitudes and the phase shift between the excitation and emission light. The resulting polarized emission components are modulated at the same frequency but phase shifted with phase decay  $\Phi$  relative to each other [10].

$I_{\parallel AC}$  and  $I_{\perp AC}$  are the amplitudes of  $I_{\parallel}$  and  $I_{\perp}$  in the frequency domain, respectively.  $I_{\parallel DC}$  and  $I_{\perp DC}$  are the average values of  $I_{\parallel}$  and  $I_{\perp}$ , respectively. These signals are characterized by the ratio

$$Y_{AC} = I_{\parallel AC} / I_{\perp AC}, \quad Y_{DC} = I_{\parallel DC} / I_{\perp DC} \quad (4)$$

Furthermore, the fluorescence lifetime of the emission light can be measured in the frequency domain. The fluorescence lifetime  $\tau$  is determined by both a series of data sets for the excited light intensity,  $i(\omega)$ , and the total light intensity of the emission light,  $I(\omega)$ .

The parameters  $\Phi$ ,  $Y_{AC}$ , and  $Y_{DC}$  are then related to parameters  $\bar{r}$ ,  $r_0$ ,  $r_{\infty}$  and  $\sigma$  by

$$\Phi = \tan^{-1} \left( \frac{\frac{3\sigma(r_0 - r_{\infty})}{2\sqrt{(1-r_0)(1+2r_0)}[(1-r_0)+(1-r_{\infty})\sigma]}}{\sqrt{[(1+2r_0)+(1+2r_{\infty})\sigma]}} \right) \quad (5)$$

$$Y_{AC} = \sqrt{\frac{(1+2r_0)^2(\omega\tau)^2 + [(1+2r_0)+(1+2r_{\infty})\sigma]^2}{(1-r_0)^2(\omega\tau)^2 + [(1-r_0)+(1-r_{\infty})\sigma]^2}} \quad (6)$$

$$Y_{DC} = \frac{(1+2r_0)+(1+2r_{\infty})\sigma}{(1-r_0)+(1-r_{\infty})\sigma} \quad (7)$$

$$\bar{r} = \frac{Y_{DC} - 1}{Y_{DC} + 2} \quad (8)$$

The rotational correlation time  $\theta$  is given by

$$\theta = \left[ \frac{Y_{AC} \left[ (Y_{AC}^2 - 2Y_{DC})(Y_{DC} + 2)\sqrt{1 + \tan^2 \Phi} + Y_{AC}(Y_{DC} - 4) \right] \tan(\Phi \cdot \omega\tau)}{(Y_{AC}^2 - 4)(Y_{AC}^2 - Y_{DC}^2) + (Y_{AC}^2 - 2Y_{DC})^2} \right]^{-1} \tau \quad (9)$$

To define the rotational correlation time  $\theta$ , the fluorescence lifetime  $\tau$  is required.

The fluorescence lifetime  $\tau$  is determined by the phase decay  $\delta$  and modulation  $m$  of the fluorescence, which is excited using light whose intensity  $i(t)$  varies sinusoidal with time [10]:

$$i(t) = a + b \sin(\omega t) \quad (10)$$

where  $\omega$  is the angular velocity of the modulated excitation light [10]. As a consequence of the finite duration of the excited state, the modulated fluorescence emission is delayed in phase by angle  $\delta$  relative to the excitation. In addition, the modulation of the fluorescence decreases. The intensity of the fluorescence is given by

$$I(t) = A + B \sin(\omega t - \delta). \quad (11)$$

We acquire the phase decay  $\delta$  between the sinusoidal curve of the excitation light and the emitted fluorescence without the emission polarizer in the frequency domain by

$$\tan \delta = \omega \tau. \quad (12)$$

## 2.2. Particle sizing using sphere model

For Brownian particles reorienting in a liquid, the Debye model defines an exponential decay for the single-particle orientation time correlation function  $C$  and rotational correlation time  $\theta$ :

$$C = \exp(-t / \theta), \quad (13)$$

$$\theta = \frac{1}{6D_r}, \quad (14)$$

where  $D_r$  is the rotational diffusion coefficient.  $D_r$  is coupled with the shear viscosity  $\eta$  at temperature  $T$  using the DSE relationship [8, 9]:

$$D_r = \frac{k_B T}{V_H \eta} \quad (15)$$

where  $k_B$  is the Boltzmann constant. The hydrodynamic volume  $V_H$  is related to the particle volume  $v$  through a factor that depends on the shape of the reorienting particle and the boundary conditions. The particle volume  $v$  can be calculated by measuring the rotational diffusion coefficient  $D_r$  when the relation between  $V_H$  and  $v$  is formulated. For example, the formula for a sphere,  $V_H = 6v$ , is applied to the stick boundary conditions. The DSE relationship is known to be effective at the molecular length scales of low-viscosity liquids.

Consequently, the hydrodynamic volume  $V_H$  of a fluorophore can be determined using  $\Phi$ ,  $Y_{AG}$ ,  $Y_{DG}$ ,  $\omega$ , and  $\tau$  on the basis of Eqs. (14), Eq. (15), and (12). When the sphere approximation is applied to a fluorophore–nanoparticle conjugate, the diameter can be calculated from  $V_H$ . This reflects the excited state lifetime and intrinsic rotational diffusion properties of the fluorophore and the modulation frequency.

## 3. EXPERIMENTAL SETUP

We developed a rotational diffusion coefficient measurement system using an FP method, as shown in Figure 2. An Ar<sup>+</sup> laser (wavelength: 488 nm) is the polarized light source, and it is coupled to an acousto-optic modulator (AOM). Before coupling to the AOM, the polarization direction is oriented using a half-wave plate (1/2 WP) to improve the diffraction efficiency of the AOM. High-speed light amplitude modulation (up to 80 MHz) can be achieved in the unit, which consists of the AOM, lens (L), and iris.

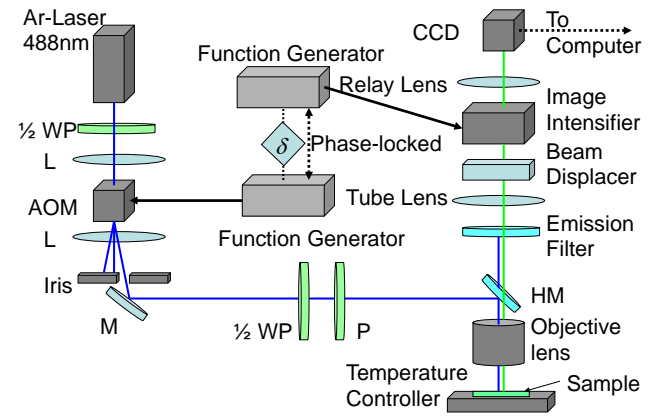


Figure 2. Experimental setup.

The polarization direction of the input signal is then oriented by a half-wave plate (1/2 WP) just as with the polarization direction of  $I_{||}$ . The light is incident on the sample via a half mirror (HM) and objective lens. The sample is excited using linearly polarized light. The emission is relayed through the beam displacer, which divides the fluorescence polarization signals oriented parallel ( $I_{||}$ ) and perpendicular ( $I_{\perp}$ ) to the excitation beam polarizer. The fluorescence signals are finally relayed to the image intensifier. The image of the orthogonal components of the fluorescence signal is enhanced on the image intensifier and then relayed to a CCD. Images of both the horizontally ( $I_{||}$ ) and vertically ( $I_{\perp}$ ) polarized components are analyzed to acquire the fluorescence anisotropy. The modulation of the gain of the image intensifier corresponds to the modulation of the input signal amplitude. The phase decay  $\delta$ , is the phase difference between the incident light and the gain of the image intensifier. Acquisition proceeds with a series of phase shifts to acquire a first-order photo bleaching compensation. A data series is processed to yield the frequency-dependent amplitudes, along with the phase shift between the excitation light and the emitted lights in the two orthogonal polarization directions. The polarized emission components are modulated at the same frequency but phase shifted relative to each other.

## 4. EXPERIMENTAL RESULTS

### 4.1. Rotational correlation time for fluorophore

To measure the particle sizes, precise measurement of the rotational diffusion coefficient, which corresponds to the rotational correlation time, is required, as shown in Eq. (14). We performed fundamental experiments to verify the feasibility of

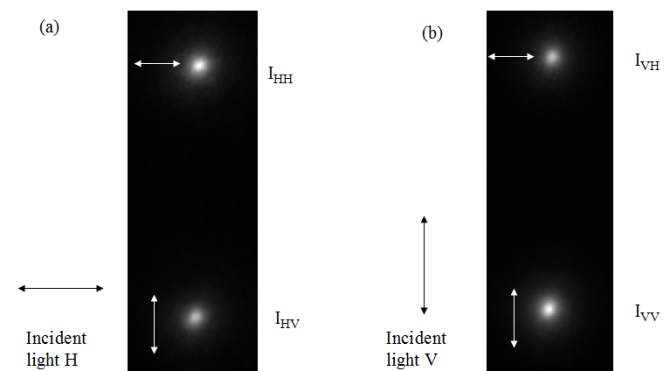


Figure 3. CCD images of fluorescence signals.

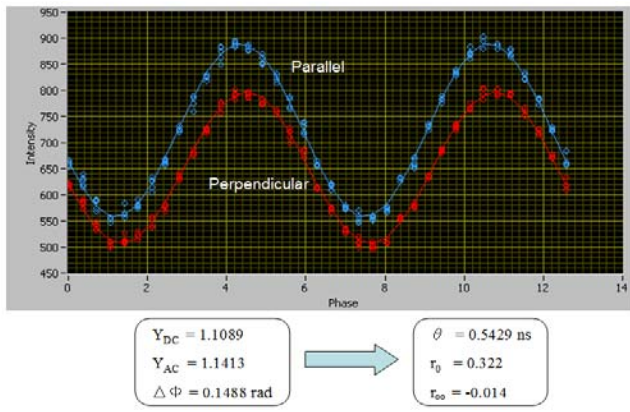


Figure 4. Parallel and perpendicular polarized components of modulated fluorescence signal.

precise measurement of the rotational correlation time for the fluorophore [11] without labeling gold nanoparticles.

In the experiment, a beam displacer is used to divide the fluorescence light into the parallel and perpendicular components. As shown in Figure 3, both components of the signal are observed in the CCD camera after the fluorescence light passes through the beam displacer. The upper component is polarized in the horizontal (H) direction, and the lower component is polarized in the vertical (V) direction. To check the efficiency of both sides, two measurements are required. First, the polarization angle of the excitation light is adjusted to the direction parallel to the horizontal direction, and an image is recorded, as shown in Figure 3(a). The intensities of the horizontal and vertical signals are denoted by  $I_{HH}$  and  $I_{HV}$ , respectively. Next, the polarization angle of the excitation light is adjusted to the direction parallel to the vertical direction, and another image is recorded. The intensities of the horizontal and vertical signals are also denoted by  $I_{VH}$  and  $I_{VV}$ , against the orthogonal direction of polarization respectively, as shown in Figure 3(b). Fifteen images are taken for each case. Depending on the direction of polarization, the efficiency of the light passing through may differ. Therefore, a calibration factor  $G$  is needed to measure  $I_{\parallel}$  and  $I_{\perp}$  from the two signal components. We calculated the  $G$  factor for  $I_{VH}$ ; thus, when excitation light in the V direction is used,  $I_{VV}$  is used directly in our calculation, and  $I_{VH}$  times  $G$  is used for the H direction of  $I_{\parallel}$ . The  $G$  factor for  $I_{VH}$  is obtained as follows:

$$G_{I_{VH}} = \sqrt{\frac{I_{VV}I_{HV}}{I_{VH}I_{HH}}} \quad (16)$$

The modulation frequency of the AOM was set to 60 MHz for the following experiment. The CCD exposure time was 400 ms, and the micro channel plate voltage was 760 V. The modulated fluorescence signals by varying the phase  $\Phi$  are

$$\theta = \frac{Y_{AC}^2(1-r_{\infty})^2 - (1+2r_{\infty})^2}{(1+2r_0)(1+2r_{\infty}) - Y_{AC}^2(1-r_0)(1-r_{\infty}) + \sqrt{Y_{AC}^2 \left[ 9(r-r_{\infty})^2 + \left\{ \begin{array}{l} 2+r_{\infty}(2+5r_{\infty}) + r_0[2-4r_{\infty}(4+r_{\infty})] + \\ +r_0^2[5-4r_{\infty}(1-2r_{\infty})] - Y_{AC}^2(1-r_0)^2(1-r_{\infty})^2 \end{array} \right\} (\omega\tau)^2 \right]} - (1+2r_0)^2(1+2r_{\infty})^2 (\omega\tau)^2} \cdot \tau \quad (18)$$

$$D_r = \frac{1+2r_0 - Y_{AC}^2(1-r_0) + \sqrt{Y_{AC}^2 \left[ 9r_0^2 + \left\{ 2+2r_0 + 5r_0^2 - Y_{AC}^2(1-r_0)^2 \right\} (\omega\tau)^2 \right]} - (1+2r_0)^2 (\omega\tau)^2}{6(Y_{AC}^2 - 1)\tau} \quad (19)$$

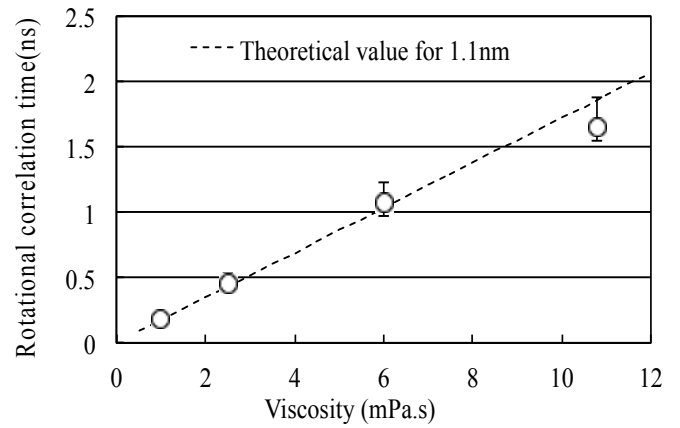


Figure 5. Rotational correlation time of fluorophore.

shown in Figure 4.  $\Phi$ ,  $Y_{AC}$ , and  $Y_{DC}$  are determined from the fitting curves of both fluorescence signals.

First, the fluorescence anisotropy as a function of the time  $t$  is evaluated using the developed system. Figure 5 shows the linear variation in the rotational correlation time versus the viscosity of the solution. Three solutions were prepared for measuring the rotational correlation time of a fluorophore by mixing water with glycerin at 30 wt%, 50 wt%, and 60 wt%. The resulting viscosities were 2.5 mPa·s, 6.0 mPa·s, and 10.8 mPa·s at 293 K, respectively. We also used water, which has a viscosity of 1.0 mPa·s at 293 K, as a solution. The fluorophore was Alexa Fluore 488 (Invitrogen Corp.), which is the same size as fluorescein. The fluorescence lifetime  $\tau$  varies, with values of 4.1 ns in water, 3.8 ns in 30 wt% glycerin, 3.6 ns in 50 wt% glycerin, and 3.1 ns in 60 wt% glycerin.

If we apply the sphere approximation for the fluorophore, the theoretical value of the rotational correlation time, which depends on the particle size, can be calculated from Eqs. (14) and (15) as follows:

$$\theta = \frac{6\pi d^3 \eta}{k_B T} \quad (17)$$

The theoretical value is plotted according to the solution temperature  $T$  (293 K) and nanoparticle diameter  $d$  (1.1 nm). According to Eq. (16), the rotational correlation time of the fluorophore agrees well with the value for a nanoparticle with a diameter of 1.1 nm under the nonslip boundary condition. This value is close to that of fluorescein, whose size is estimated to be 1.0 nm [12, 13]. The size difference is considered to be an effect of hydration of the fluorophore in the solution. From the above results, the rotational correlation time can be precisely measured using the developed system.

#### 4.2. Rotational diffusion coefficient for gold nanoparticle with

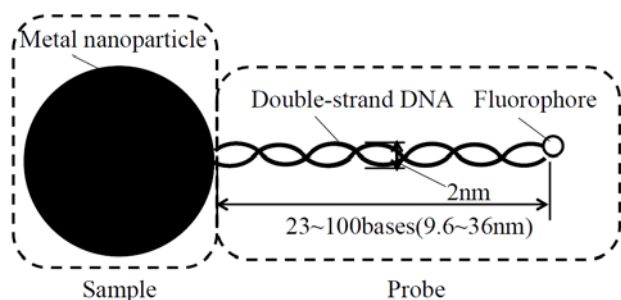


Figure 6. Distance between gold nanoparticle and fluorescent probe.

### fluorescent DNA probe

To evaluate the diameter of a gold nanoparticle, the rotational diffusion coefficient of the nanoparticle with a fluorescent DNA probe is evaluated using the developed system. Gold nanoparticles with average diameters of 8.2 nm were prepared as the standard sample for measurement of the rotational diffusion coefficient. We evaluated the rotational diffusion coefficient of the gold nanoparticles directly with the fluorescent DNA probe.

The fluorescent probe was connected to the gold nanoparticles via double-strand DNA consisting of adenine with a length of 23 bases. The length of the double-strand DNA is estimated to be 9.6 nm, as shown in Figure 6. The DNA acts as a spacer to avoid quenching of the fluorophore [14, 15, 16], which is located near the gold nanoparticle. The 23-base double-strand DNA is strong enough to avoid bending [17, 18] and to maintain the distance between the gold nanoparticle and fluorophore.

Figure 7 shows the rotational diffusion coefficient of the fluorophore and gold nanoparticle with the fluorescent DNA probes versus the solution parameters, represented by  $T/\eta$ . The rotational correlation time  $\theta$  is calculated using Eq. (18) and the data for the parameters  $\Phi$ ,  $Y_{AC}$  and  $Y_{DC}$ .

The rotational diffusion coefficient can be calculated using the reciprocal of  $\theta$ , as shown in Eq. (19). Table 1 shows the measurement parameters used to evaluate the rotational diffusion coefficient.

As shown in Figure 7, the rotational diffusion coefficient, which indicates the speed of rotational motion, increases linearly with  $T/\eta$ . This relation agrees with Eq. (17), which shows a linear relation to  $\eta/T$ .

The inclination of the graph for the rotational diffusion coefficient of the fluorescent DNA probe is four times higher than that of the gold nanoparticle (average diameter, 8.2 nm) with the fluorescent DNA probe. A large difference in the rotational correlation coefficient appears between the fluorescent DNA probe and the gold nanoparticle with the probe. This enables us to estimate the size of a gold

Table 1. Measurement parameters.

Temperature [K]	Viscosity [mPa·s]	Probe		Probe + gold nanoparticle	
		$\tau$ [ns]	$Y_{AC}$	$\tau$ [ns]	$Y_{AC}$
293	1.002		1.225		1.457
298	0.890		1.199		1.435
303	0.797	2.0	1.172	1.0	1.427
308	0.719		1.151		1.402
313	0.653		1.135		1.396

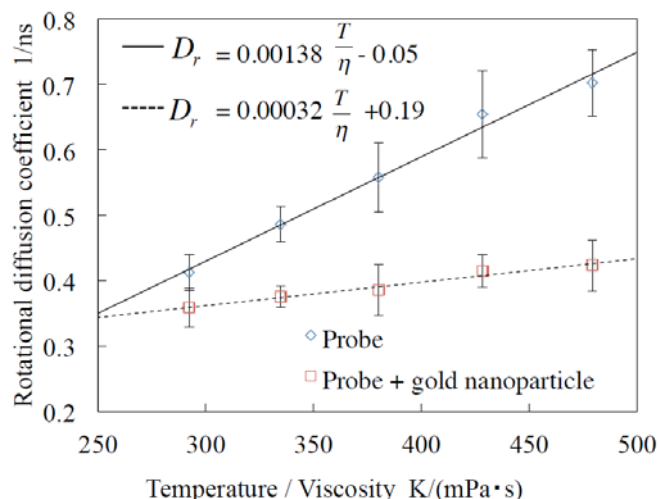


Figure 7. Rotational diffusion coefficients for fluorophore and gold nanoparticle with fluorescent DNA probe.

nanoparticle quantitatively using the inclination of the rotational diffusion coefficient against the viscosity of the temperature.

To evaluate the resolution of the particle sizing obtained using the proposed method, further experiments for various diameters of gold nanoparticles are needed. We are now preparing samples of gold nanoparticles with average diameters of 5 nm, 10 nm, 15 nm, and 20 nm.

## 5. CONCLUSIONS

We developed a nanoparticle sizing system using an FP method. This system can precisely determine the rotational correlation time of nanoparticles with a fluorophore. The results indicate that we can determine the size of a nanoparticle using the DSE relation when the particle shape approximates a sphere.

We also investigated the rotational correlation time of a fluorophore with gold nanoparticles that were smaller than 10 nm. This indicates that the measurement results for the rotational correlation time of a fluorophore-labeled gold particle can be used to estimate the size of gold nanoparticles smaller than 10 nm.

## ACKNOWLEDGMENT

This research was supported in part by a Grant-in-Aid for Scientific Research from the Ministry of Education, Culture, Sports, Science and Technology of Japan (Grant-in-Aid for Exploratory Research 21686015).

## REFERENCES

- [1] T. Gao, Q. Li, and T. Wang, "Sonochemical synthesis, optical properties, and electrical properties of core/shell-type ZnO nanorod/CdS nanoparticle composites," *Chem. Mater.*, no. 17, pp. 887–892, 2005.
- [2] R. G. Freeman, K. C. Grabar, K. J. Allison, R. M. Bright, J. A. Davis, A. P. Guthrie, M. B. Hommer, M. A. Jackson, P. C. Smith, D. G. Walter, and M. J. Natan, "Self-assembled metal colloid monolayers: an approach to SERS substrates," *Science*, vol. 267, no. 5204, pp. 1629–1632, 1995.
- [3] S. Sun, C. B. Murray, D. Weller, L. Folks, and A. Moser, "Monodisperse FePt nanoparticles and ferromagnetic FePt nanocrystal superlattices," *Science*, vol. 287, no. 5460, pp. 1989–1992, 2000.

- [4] R. Pecora, "Dynamic light scattering measurement of nanometer particles in liquids," *J. Nanopart. Res.*, vol. 2, issue 2, pp. 123-131, 2000.
- [5] L. C. Gontard, D. Ozkaya, and R. E. Dunin-Borkowski, "A simple algorithm for measuring particle size distributions on an uneven background from TEM images," *Ultramicroscopy*, vol. 111, issue 2, pp. 101-106, 2011.
- [6] K. Kinoshita Jr., S. Kawato, and A. Ikegami, "A theory of fluorescence polarization decay in membranes," *Biophys. J.*, vol. 20, issue 3, pp. 289-305, 1977.
- [7] B. S. Fujimoto and J. M. Schurr, "An analysis of steady-state fluorescence polarization anisotropy measurements on dyes intercalated in DNA," *J. Phys. Chem.*, vol. 91, no. 7, pp. 1947-1951, 1987.
- [8] F. Stickel, E. W. Fischer, and R. Richert, "Dynamics of glass-forming liquids. II. Detailed comparison of dielectric relaxation, dc-conductivity, and viscosity data," *J. Chem. Phys.*, vol. 5, no. 104, pp. 2043-2055, 1996.
- [9] P. P. Jose, D. Chakrabarti, and B. Bagchi, "Complete breakdown of the Debye model of rotational relaxation near the isotropic-nematic phase boundary: Effects of intermolecular correlations in orientational dynamics," *Phys. Rev. E*, no. 73, 031705, 2006.
- [10] R. F. Steiner, "Fluorescence anisotropy: Theory and applications," *Top. Fluoresc. Spectrosc.*, vol. 2, pp. 1-52, 1991.
- [11] M. B. Mustafa, D. L. Tipton, M. D. Barkley, and P. S. Russo, "Dye diffusion in isotropic and liquid crystalline aqueous (hydroxypropyl) cellulose," *Macromolecules*, vol. 26, no. 2, pp. 370-378, 1993.
- [12] A. H. A. Clayton, Q. S. Hanley, D. J. Arndt-Jovin, V. Subramaniam, and T. M. Jovin, "Dynamic fluorescence anisotropy imaging microscopy in the frequency domain (rFLIM)," *Biophys. J.*, vol. 83, pp. 1631-1649, 2002.
- [13] R. D. Spencer and G. Weber, "Measurement of subnanosecond fluorescence lifetimes with a cross-correlation phase fluorometer," *Ann. N. Y. Acad. Sci.*, vol. 158, no. 1, pp. 361-376, 1969.
- [14] C. S. Yun, A. Javier, T. Jennings, M. Fisher, S. Hira, S. Peterson, B. Hopkins, N. O. Reich, and G. F. Strouse, "Nanometal surface energy transfer in optical rulers, breaking the FRET barrier," *J. Am. Chem. Soc.*, vol. 127, no. 9, pp. 3115-3119, 2005.
- [15] J. Seelig, K. Leslie, A. Renn, S. Kühn, V. Jacobsen, M. van de Corput, C. Wyman, and V. Sandoghdar, "Nanoparticle-induced fluorescence lifetime modification as nanoscopic ruler: demonstration at the single molecule level," *Nano Lett.*, vol. 7, no. 3, pp. 685-689, 2007.
- [16] S. Mayilo, M. A. Kloster, M. Wunderlich, A. Lutich, T. A. Klar, A. Nichtl, K. Kürzinger, F. D. Stefani, and J. Feldmann, "Long-range fluorescence quenching by gold nanoparticles in a sandwich immunoassay for cardiac troponin T," *Nano Lett.*, vol. 9, no. 12, pp. 4558-4563, 2009.
- [17] D. Porschke, "Persistence length and bending dynamics of DNA from electrooptical measurements at high salt concentrations," *Biophys. Chem.*, vol. 40, issue 2, pp. 169-179, 1991.
- [18] G. S. Manning, "The persistence length of DNA is reached from the persistence length of its null isomer through an internal electrostatic stretching force," *Biophys. J.*, vol. 91, no. 10, pp. 3607-3616, 2006.